Local ancestry prediction with *PyLAE*

Nikita Moshkov [Equal first author, 1, 2, 3, 4] , **Aleksandr Smetanin** [Equal first author, 5] , **Tatiana V Tatarinova** [Corresp. 6, 7, 8, 9]

1 Biological Research Centre,, Szeged, Hungary

2 University of Szeged, Szeged, Hungary

3 National Research University Higher School of Economics, ,, Moscow, Russia

4 Tintagel House, 92 Albert Embankment, Lambeth, Atlas Biomed Group Limited, London, SE1 7TY, United Kingdom

5 ITMO University, Saint-Petersburg, Russia

6 Department of Biology, University of La Verne, La Verne, CA, United States

7 Siberian Federal University, Krasnoyarsk, Russia

8 Institute of General Genetics, Moscow, Russia, Moscow, Russia

9 Institute for Information Transmission Problems, Moscow, Russia, Moscow, Russia

Corresponding Author: Tatiana V Tatarinova
Email address: ttatarinova@laverne.edu

Summary. We developed *PyLAE* - a new tool for determining local ancestry along a genome using whole-genome sequencing data or high-density genotyping experiments. PyLAE can process an arbitrarily large number of ancestral populations (with or without an informative prior). Since *PyLAE* does not involve estimating many parameters, it can process thousands of genomes within a day. *PyLAE* can run on phased or unphased genomic data. We have shown how *PyLAE* can be applied to the identification of differentially enriched pathways between populations. The local ancestry approach results in higher enrichment scores compared to whole-genome approaches. We benchmarked PyLAE using the 1000 Genomes dataset, comparing the aggregated predictions with the global admixture results and the current gold standard program RFMix. Computational efficiency, minimal requirements for data pre-processing, straightforward presentation of results, and ease of installation make *PyLAE* a valuable tool to study admixed populations. **Availability and implementation**. The source code and installation manual are available at https://github.com/smetam/pylae.

1 Local Ancestry Prediction with *PyLAE*

2 Nikita Moshkov [1-4], Alexander Smetanin [5], Tatiana V. Tatarinova [6-9]

4 *[1] Biological Research Centre, Szeged, Hungary*

5 *[2] University of Szeged, Szeged, Hungary*

6 *[3] National Research University Higher School of Economics, Moscow, Russia*

7 *[4] Atlas Biomed Group Limited, Tintagel House, 92 Albert Embankment, Lambeth, SE1 7TY,*

8 *London, United Kingdom*

9 *[5] ITMO University, Saint-Petersburg, Russia*

10 *[6] Department of Biology, University of La Verne, La Verne, California, USA*

11 *[7] Siberian Federal University, Krasnoyarsk, Russia*

12 *[8] Institute for Information Transmission Problems, Moscow, Russia*

13 *[9] Institute of General Genetics, Moscow, Russia*

Abstract

15 **Summary.** We developed *PyLAE* - a new tool for determining local ancestry along a
16 genome using whole-genome sequencing data or high-density genotyping experiments. *PyLAE*
17 can process an arbitrarily large number of ancestral populations (with or without an informative
18 prior). Since *PyLAE* does not involve estimating many parameters, it can process thousands of
19 genomes within a day. *PyLAE* can run on phased or unphased genomic data.

20 We have shown how *PyLAE* can be applied to the identification of differentially enriched
21 pathways between populations. The local ancestry approach results in higher enrichment scores
22 compared to whole-genome approaches.

23 We benchmarked *PyLAE* using the 1000 Genomes dataset, comparing the aggregated
24 predictions with the global admixture results and the current gold standard program RFMix.
25 Computational efficiency, minimal requirements for data pre-processing, straightforward
26 presentation of results, and ease of installation make *PyLAE* a valuable tool to study admixed
27 populations.

28 **Availability and implementation**. The source code and installation manual are available
29 at https://github.com/smetam/*PyLAE*.

Introduction

32 In association studies, researchers combine samples with different (usually opposing)
33 phenotypes and compare Single Nucleotide Polymorphisms (SNPs) frequencies in two groups.
34 When enough samples are available (typically, thousands for complex traits), a significant

35 difference in frequencies between the groups suggests an association between the position on
36 the genome and the studied phenotype. However, there is a possibility that the association is due
37 to inhomogeneity of the study group in terms of provenance/origin (for example, all people with
38 the disease are of French origin, and the healthy cohort is Bulgarian). In this case, two populations
39 may have different frequencies of ancestry informative markers (AIM) that are not causal to the
40 phenotype.
41   An intuitive approach to solving this problem is determining the population structure first
42 and then adjusting for it. However, this strategy is complicated for admixed populations. Due to
43 meiotic recombination during transmission of genetic material to the offspring, individual
44 segments of the genome may have different origins. Recombination makes it hard to determine
45 the source of such individuals (or plant populations), especially locus-specific local origin.
46   Several solutions to this problem exist, such as (LAMP, LAMP-ANC, and RFMIX).
47 However, there is always room to develop a user-friendly, fast, accurate approach. LAMP
48 (Sankararaman et al., 2008) algorithm determines local origin in mixed populations. The LAMP
49 input includes the recombination rate, global mixing ratio, and the number of generations that
50 have passed since the mixing started. The recombination rate can be considered known due to
51 previous studies (Nachman & Crowell, 2000), while the global proportion can be estimated using,
52 for example, the ADMIXTURE tool (Alexander, Novembre & Lange, 2009). The idea of the LAMP
53 method is as follows. The iterated conditional modes clustering algorithm (ICM) determines the
54 likelihood that a genome segment within a selected window has a specific origin. An individual
55 SNP is assigned the source by the "popular vote" approach using the inferred origins of all
56 windows covering this position. ICM is a modification of the Expectation-Maximization (EM)
57 algorithm, which receives a point estimate at the E-step under the assumption that the a priori
58 estimates are sufficiently accurate. Therefore, the ICM is faster than the EM approach. To
59 construct an accurate *a priori* estimate, LAMP uses the MAXVAR algorithm, which works only for
60 two populations. The size of the genomic window is selected to minimize classification errors.
61 LAMP works fast, but its accuracy decreases if the ethnic admixture ratio is close to 1:1.
62   LAMP-ANC (Pasaniuc et al., 2009) is a modification of the LAMP tool, showing a higher
63 accuracy than LAMP. This modification also allows triple mixing to be estimated, while LAMP
64 cannot determine frequencies for more than two ancestral populations.
65   Machine Learning algorithm RFMIX (Maples et al., 2013; Uren, Hoal & Möller, 2020) treats
66 origin as a hidden parameter in its statistical model. RFMIX employs conditional random fields
67 and decision trees. The RFMIX model does not impose restrictions on the number of ancestral
68 populations and types of mixing.
69   We developed *PyLAE* - a new tool for determining local origin along a genome using
70 whole-genome sequencing data or high-density genotyping experiments. *PyLAE* can process an
71 arbitrarily large number of ancestral populations (with or without an informative prior). *PyLAE* does
72 not involve the estimation of many parameters. *PyLAE* is a valuable tool to study admixed
73 populations (Hester et al., 2011; N'Diaye et al., 2011; Kantor et al., 2013). We have tested this
74 approach using the 1000 Genomes database.
75

Materials and Methods

Data source

Whole-genome sequencing data in the VCF format were obtained from the 1000 genomes project (ftp://ftp.1000genomes.ebi.ac.uk/vol1/ftp/, genome version GRCh37). We used the dataset of 2504 worldwide individuals with the reported ethnic origin (Sudmant et al., 2015) and phased genome sequence data.

Data pre-processing

Admixture

To confirm the reported origin, we have extracted 130,000 ancestry informative markers identified by a worldwide study contacted by the National Genographic consortium, as described in (Elhaik et al., 2014). The supervised admixture analysis was performed using the K=9 component division of ancestral populations into the following categories: North-East Asian, Mediterranean, South African, South-West Asian, Native American, Oceanian, Southeast Asian, Northern European, and Sub-Saharan African components. We used the putative ancestral populations from our earlier study (Elhaik et al., 2014). The admixture components represent proportions of an individual's genotype attributed to each of the nine putative ancestral genomes. The obtained nine-dimensional vectors were clustered based on the L2 norm (Euclidean distance). The optimal number of clusters was determined using the weighted Kullback-Leibler distance approach (Tatarinova, Bouck & Schumitzky, 2008; Tatarinova & Schumitzky, 2014). Within each group, the admixture profiles of individuals are similar. This dimension-reduction step allows the identification of potentially admixed individuals. This assignment was validated using haplogroup information and reAdmix analysis in group mode (Kozlov et al., 2015). reAdmix algorithm represents an individual as a weighted sum of present-day populations (e.g., 50% British, 25% Russian, 25% Han Chinese) based on K admixture components. Instead of solving an "exact admixture" problem, we aim to find the smallest subset of populations whose combined admixture components are close to those of the individuals within a small tolerance margin. Due to the range of natural variation, the admixture proportions can be considered exact neither for the reference populations nor for the tested individuals. The admixture proportions we use are merely maximum likelihood estimates and may fail to be exactly equal to the actual shares of ancestral genomes. Therefore, determining ethnic proportions is mathematically and computationally more challenging than finding a single most fitting bio-origin. From our experience with reAdmix, this tool accurately identifies all significant components; however, small proportions are frequently misassigned. When similar individuals are analyzed as a group, it is possible to estimate even the small proportions reliably.

111 Phasing

112 The phased data were obtained for the 1000 genomes from the open repository
113 ftp://ftp.1000genomes.ebi.ac.uk/vol1/ftp/. Sudmant et al. (Sudmant et al., 2015) used short-read
114 Illumina DNA sequencing data to infer haplotype blocks in 26 human populations.
115

116 Two modes

117 We have developed two modes: "diploid" and "haploid." For the "diploid" mode, we used the
118 samples without pre-processing. For the "haploid" mode, we used the phasing information
119 provided by the 1000 Genomes and assumed that the parents were homozygous and simulated
120 two homozygous "parents" for each sample. The admixture vector, used as an informative prior
121 for "diploid" and "haploid" modes, is generated by applying the Admixture tool (Alexander,
122 Novembre & Lange, 2009) to the original "diploid" sample in supervised mode.

123 # Local Ancestry Bayesian Approach (*PyLAE*)

124 **Input**:
125   **Tested Individual**: VCF file and (optional) admixture vector obtained by Admixture in
126 supervised mode, as described above.
127   **Reference**: multi VCF file with putative ancestral populations corresponding to K
128 component admixture.
129   *N* is the number of positions overlapping between the reference and the individual.
130

131 The number of genomic positions should be significantly large to ensure dense SNP coverage,
132 while not being too large since the markers should be uncorrelated. Therefore, we recommend
133 removing positions based on high levels of pairwise linkage disequilibrium (LD-pruning). It is a
134 common practice to exclude positions with pairwise genotypic $r^2 > 0.8$ within sliding windows of
135 50 SNPs (Alexander, Novembre & Lange, 2009).
136

137 **Stage 1. Bayesian posterior probability**
138 Posterior probability $P(population|genotype)$ is calculated using the Bayes formula:
139

140 $$P(Population|genotype) = \frac{P(Population|genotype)}{P(genotype)} = \frac{P(Population \cap genotype)}{P(genotype)} = \frac{P(Population)\,P(genotype|Population)}{P(genotype)}$$

141 $$= \frac{P(Population)\,P(genotype|Population)}{\sum_{k=1}^{K}P(genotype|Population_k)P(Population_k)}.$$

142

143

144 The prior probability of a population $P(population)$ is equal to the analyzed individual's admixture
145 vector. We assume that adjacent positions have the same origin and the origin of all positions
146 within a window of length **L**. Since the distance between two consecutive ancestry informative
147 markers is sufficiently large, positions within the same window can be considered independent.

148 $$P(\{genotype_1...genotype_L\}|\,population) = \prod_{i=1}^{L}P(genotype_i|population)$$

149 Therefore

150 $$P(population|genotype) = \frac{P(population)}{P(genotype)} \cdot \prod_{i=1}^{L} P(genotype_i | population)$$

151 $P(genotype_i|population)$ is estimated from observations, using genotypes of putative ancestral

152 populations in position i

153 $P(genotype) = \sum_{k=1}^{K} P(genotype|Population_k)P(Population_k)$

154 Therefore, we have K posterior probabilities for every genotype, and the matrix of posterior

155 probabilities $T \times K$, where $T = \frac{N}{L}$.

156

157 We are interested in determining the optimal sequence of the source populations along the

158 genome. This problem is solved using the Viterbi algorithm (Viterbi, 1967). For computational

159 efficiency, all calculations are performed in the log-space.

160

161 **Stage 2. Viterbi algorithm**

162

163 Our state-space *S* consists of *K* ancestral populations. Population labels (*i=1..K*) are the hidden

164 states in our model. The initial probabilities π_i of being in the ith hidden state can either be

165 assumed to be uniform with 1/K probability of each population or set to be equal to global

166 admixture components. Transition probabilities $\alpha_{i,j}$ of transitioning from the state *i* to *j* are

167 inversely proportional to the TreeMix distances between corresponding ancestral populations.

168 Transition probability from state *i* to *j* a_{ij} can be calculated from distances between ancestral

169 populations; alternatively, the same value can be used for all pairs of populations. The emission

170 probabilities $b_j(O)$ is calculated by the Bayes formula (above). At the first step of the algorithm δ_j

171 $(1) = \pi_j b_j(O_1)$. At each next step $\delta_j(t+1) = max_i \delta_i(t) a_{ij}(O_{t+1})$. The pointers $D_j(t+1)$ are

172 stored for tracing back. $D_j(t+1) = argmax_i \delta_i(t) a_{ij}(O_{t+1})$. At the terminal state: $S_T = argmax_i\delta_i$

173 (T), $S_t = D_{S_{t+1}}(t+1)$.

174

175 For efficiency, the computation is performed in the log-space. The algorithm is implemented as a

176 python script and can be adapted to analyze any organism using user-provided ancestral

177 components, prior probabilities, and transition matrix.

178 ## Application of Local Ancestry

179 Most of the currently living individuals are admixed to various degrees. To compare genotypes

180 between populations and analyze selection signals, it is essential to identify and exclude

181 introgressed regions containing non-representative genotypes. We have determined local

182 ancestry profiles for all 2504 analyzed individuals from the 1000 Genomes project. With our

183 approach, even the admixed individuals that are typically excluded from the analysis (therefore,

184 reducing the statistical power of the study) can be retained after masking the introgressed regions.

185 We have used the approach of Chekalin et al. (Chekalin et al., 2019; Benítez-Burraco et

186 al., 2021) and annotated the VCFs with the ANNOVAR tool (Wang, Li & Hakonarson, 2010; Yang

187 & Wang, 2015) using the hg19 human genome annotation and the refGene database

188 (http://varianttools.sourceforge.net/Annotation/RefGene). The SNPs were classified by their

189 location and function: 58% intergenic, 38% intronic, 5% ncRNA, and 1% exonic (64% of them are

190 synonymous, and 36% are nonsynonymous). Next, we counted the synonymous and
191 nonsynonymous SNPs per each KEGG pathway (Ogata et al., 1999; Kanehisa, 2019; Kanehisa
192 et al., 2019).
193   It is reasonable to assume that pathways accumulate nonsynonymous SNPs at the same
194 rate during neutral evolution; therefore, the pathways' enrichment scores can be approximated by
195 a normal distribution. The pathways under selection will appear as outliers.
196   To analyze differences in numbers of SNPs per pathway between the two groups of
197 populations (groups A and B), we need to calculate: 1) DSSE scores (synonymous) and 2) DNSE
198 scores (nonsynonymous) (Chekalin et al., 2019). Therefore, we perform the following steps:
199   1) Find the number of (non)synonymous SNPs in groups A and B.
200   a) Let I represent the total number of studied pathways, and $i = 1,…,I,$ be the number
201   of the (non)synonymous SNP per i^{th} pathway are nS(i) and nA(i). The expected
202   fraction of (non)synonymous SNPs in individuals from group A is given by $p =$
203             $\frac{nA}{nB + nA}$, where nA is the amount of (non)synonymous SNPs in all KEGG pathways
204   found in group A, nB is the amount of (non) synonymous SNPs in all KEGG
205   pathways found in group B. The fraction p_i of A (non)synonymous SNPs in the ith
206   KEGG pathway is $p_i = \frac{nA(i)}{nB(i) + nA(i)}.$
207   2) The enrichment D(N)SE scores are computed for every pathway with continuity correction:
208   a) $D(N/S)SE\ Score = \dfrac{(p - p_i) \pm \frac{1}{2(nS(i) + nA(i))}}{\sqrt{\frac{p(1-p)}{(nS(i) + nA(i))}}}$
209   3) P-values are calculated using Bonferroni and Benjamini–Hochberg corrections and used
210   to identify differentially enriched pathways. A pathway is considered to be differentially
211   enriched if the adjusted P-value <0.005 (Benjamin et al., 2018).
212   4) To consider the excess of synonymous SNPs over nonsynonymous SNPs, we calculate
213   enrichment scores for synonymous SNPs, DSSE. To be considered significant, the P-
214   value of the nonsynonymous test is required to be below the corresponding P-value of the
215   synonymous test for each pathway.

Using *PyLAE* with different genomes and/or sets of markers

217   A different set of putative ancestral populations or a different set of markers require
218   additional processing. First, we need to collect a database of putatively un-admixed
219   individuals. If there is an existing validated set of ancestry informative features, these
220   markers should run the admixture in supervised mode. For each self-reported ancestry,
221   samples should be clustered based on their admixture profiles to identify subgroups within
222   each self-reported ancestry. These subgroups are then examined using information about
223   the studied population's history, and the most representative subset is retained. Then,
224   putative ancestral populations (from 15 to 20 individuals per group) are generated for
225   every ancestry. The validity and stability of the ancestral populations are evaluated using
226   1) PCA, 2) leave-one-out supervised admixture, and 3) by application of supervised
227   admixture to the original dataset.
228

229 Results

230 Investigation of the reference dataset

231 An intrinsic difficulty for benchmarking an ancestry prediction pipeline is the lack of the gold
232 standard. We used the 1000 Genomes dataset for the benchmark and evaluated the quality of
233 the dataset. At first, we have investigated the 1000 Genomes dataset to determine intrinsic
234 limitations to accuracy. Our first step is a comparison between phased and unphased data. *PyLAE*
235 can process both phased and unphased data, which is both a blessing and a curse. It is a blessing
236 since some genomes may not have phased data, and it is a curse since the accuracy may suffer.
237 Therefore, we first evaluate the constraints that are imposed by different components of the
238 pipeline. The first component is the calculation of the Admixture (Alexander, Novembre & Lange,
239 2009) profiles.
240

241 Admixture profiles in Diploid vs. Haploid modes
242

243 Nine-dimensional admixture profiles were calculated for 2,504 individuals (130K markers each)
244 using supervised admixture. Every sample was analyzed first in diploid and then in haploid mode
245 (Figure 1).
246
247
248

249 Diploid and haploid admixture profiles were clustered within each reported ethnic origin (Figure
250 2, Tables 1 and 2). African Ancestry SW, African Caribbean, Columbian, Gambian Mandinka,
251 Mexican Ancestry, Peruvian, and Puerto-Rican showed 2-3 subgroups within each reported
252 ethnicity, consistent with the complex population history of these populations.
253
254
255

256
257

258 We have investigated the difference between inferred haploid parental admixture profiles and
259 diploid admixture profiles of analyzed individuals. We have computed an average of parental
260 haploid admixture vectors for every individual and calculated the Euclidean distance between the
261 vectors. The average distance for all individuals was 0.092. On average, the largest differences
262 were observed for Toscani, Iberian, Columbian, Mexican Ancestry, and Puerto Rican individuals.
263 In diploid mode, the average value of the Mediterranean component in Toscani individuals was
264 60%, South West Asian - 23%, and Northern European -15%. In haploid mode, the Mediterranean
265 component was 82%, and South-West Asian - 18%. The same situation happened with the Iberian
266 samples. In the diploid mode, the average value of the Mediterranean component was 55%, South
267 West Asian - 19%, and Northern European -24%. In the double haploid mode, the Mediterranean
268 component was 72%, South West Asian - 16%, and Northern European - 12%. Similar inflation

269 in the Mediterranean component was accompanied by a reduction in the Northern European
270 components.
271   To investigate the source of this difference, we have identified the most significant
272 admixture component for every sample and calculated the difference between the average
273 parental value of this component and its diploid value. The difference ranged from -0.0057 to
274 0.3063; the mean difference was 0.0684, indicating that haploid admixture tends to increase the
275 value of the largest component. The magnitude of the increment grows approximately linearly for
276 components <0.87 and then reduces linearly for components above 0.87. Worldwide populations
277 show different trends (Figure 3). For individuals of European and East Asian descent, the trend
278 is positive linear, and the larger the value, the more it is inflated. For South Asian individuals,
279 there is no clear trend. For African and American individuals, there are multiple linear trends. The
280 slope of the line is defined by the relative values of the admixture components. For example,
281 among Columbians, a larger slope corresponds to the individuals where the average ratio of
282 Mediterranean to the sum of Sub-Saharan African and Native American components is 2.07. In
283 comparison, a smaller slope corresponds to a 0.56 ratio.
284

285 Population-specific accuracy limitations of the admixture-based approach
286
287 We have investigated the accuracy limitations of the dataset and admixture-based approaches.
288 First, for each individual's admixture vector, we have calculated the nearest population, based on
289 Euclidean distance between admixture vectors, using the leave-one-out approach; then we have
290 computed fractions of self-hits (the nearest population agrees with the population label of the
291 individual), and fractions of super population self-hits (the agreement is at the level of super-
292 populations). Admixed populations like African American, African Caribbean, Colombian, Mexican
293 in the USA, Peruvian, and Puerto Rican have the lowest assignment accuracy at both population
294 and subpopulation levels. We also noticed that West African populations, such as Yoruba, Esan,
295 Gambian Mandinka, and Mende, are frequently misclassified. Although they speak languages
296 from the same Niger-Congo group, their genomes are not identical (Skoglund et al., 2017; Fan et
297 al., 2019). Simplified representation using nine admixture components is artificially "collapsing"
298 those groups to a single point in 9-dimensional space.
299
300
301
302
303
304 GPS and reAdmix (Table 3, Figure 4) analyses suggest that population labels were not 100%
305 accurate but were correct at the superpopulation level. For example, about 30% of Yoruba
306 individuals were mapped to Yoruba reference, but all were mapped to various African reference
307 populations. Several factors can explain this: first, there is true heterogeneity of individuals and
308 fuzzy boundaries between populations; second, there may be a human error factor on behalf of
309 the sampled individual or a researcher collecting data; the third factor is the unreported admixture
310 from different populations. Native and African American individuals appear to be the most affected

311   by these factors; this observation agrees with known historical events. Therefore, we expect to
312   see admixed regions along the genomes of affected individuals.
313
314

Performance of the *PyLAE* algorithm

316

317   We have tested the *PyLAE* algorithm on 2504 individuals of the 1000 Genomes dataset using:
318   diploid and haploid versions, with informative and noninformative priors. Informative prior is
319   assumed to be equal to the global admixture vector. The noninformative prior is uniform,
320   assuming equal probabilities for a region to be from any of the K reference populations.
321   Since we do not know the origins of regions of the genome, we chose the agreement with
322   the global admixture vector as a measure of performance. For each analyzed individual, we have
323   computed a total fraction of a genome attributed to each of the K components and compared it to
324   the global admixture vector. We have calculated Euclidean distance and Pearson correlation of
325   aggregated results and admixture vectors. The results are shown in Figure 5 and Table 4.
326

327

328   We compared *PyLAE* with the current local ancestry gold-standard tool RFMix [6]. We
329   used the 1000 Genomes dataset and have selected 150K ancestry-informative markers. *PyLAE*
330   and RFMix use different inputs and require separate data preparation steps. For RFMix, the
331   following actions were performed: (1) phase ancestral samples (2) obtain genetic maps. The
332   phasing was performed with Beagle (Browning, Zhou & Browning, 2018). *PyLAE* window size
333   was set to 15, 30, 50, and 100 SNPs; no genetic map information was used. *PyLAE* was tested
334   with the prior (results of admixture in supervised mode) and without prior, only the 'phased' case.
335   We have also tried various values of the transition penalty. The probability of changing the
336   population assignment (transition probability) was modeled as $a_{i \neq j} = \frac{1}{n+x}$, where *n* is the number
337   of populations and *x* is the penalty, that was ranged from 0 (uniform prior), to 10,000.
338   We aggregated the results according to the following rules: for *PyLAE* – we have
339   computed a fraction of windows assigned to each ancestral population; for RFMix, we have
340   calculated a fraction of markers assigned to each ancestral population. Then the results were
341   compared with the global ancestry assignments calculated by Admixture (Alexander, Novembre
342   & Lange, 2009).
343   We simulated admixed individuals with the known origin of each genomic fragment and
344   computed the fraction of correctly assigned positions. The choice of the optimal window size
345   (measured in the number of SNPs per window) is determined by the ancestral composition of the
346   analyzed sample (Figure 6). Overall, an increase in the transition penalty suppresses switches
347   between predicted populations and results in smoother prediction. Therefore, we recommend
348   using the penalty of 10,000 or higher unless there are reasons to believe that the sample is highly
349   mosaic.
350

351

352

353   Table 5 shows that for individuals with East Asian and European ancestry, *PyLAE* has a
354   higher correlation with corresponding global ancestral composition compared to RFMix. For
355   African, American, and South Asian individuals, RFMix had a higher correlation. It is important to
356   notice that global and aggregated local ancestries were in agreement for both programs; the
357   lowest correlation coefficient was 0.8676. In the 1000 Genomes dataset, African, American, and
358   South Asian samples are more admixed than East Asian and European samples.
359   *PyLAE* and RFMix have correctly determined the origin for 98.6% and 99% of genomic
360   positions across all simulated samples, respectively. Predictions made by RFMix and *PyLAE* were
361   highly concordant: the predictions agreed on 98.52% of the genome. Therefore, we propose that
362   *PyLAE* and RFMix complement each other and be used as a part of the same local ancestry
363   pipeline to improve prediction accuracy.
364
365
366

Application of Local Ancestry

367

368   Using the ANNOVAR (Wang, Li & Hakonarson, 2010; Yang & Wang, 2015) and snpEFF
369   (Cingolani et al., 2012), we have performed variation annotations and calculated the counts of
370   synonymous and nonsynonymous SNPs. We have conducted this analysis in several modes: (1)
371   comparing British, Finnish, and CEU samples with African American and African Caribbean
372   samples; (2) comparing British, Finnish, and CEU samples with all African samples; (3)
373   comparing British, Finnish, and CEU samples with African samples from Africa, selecting Northern
374   European component in European samples and Sub-Saharan African component in African
375   samples; (4) comparing British, Finnish and CEU samples with African American and African
376   Caribbean samples, selecting Northern European component in European samples and the Sub-
377   Saharan African component in African samples; (5) comparing British, Finnish and CEU samples
378   with African samples from Africa, selecting the Sub-Saharan African component in African
379   samples; (6) comparing British, Finnish and CEU samples with African Americans and the African
380   Caribbean, selecting the Sub-Saharan African component in African samples.
381   Since we use a nine-component representation, all Africans in our datasets were assigned
382   to the same Sub-Saharan African component. At the same time, African Americans have various
383   admixture levels from other components. Therefore, local ancestry mode only partitions genomes
384   of European and African American individuals.
385   On average, *PyLAE* has higher enrichment scores compared to the whole-genome
386   approach. Comparing the enrichment scores between differentially enriched pathways (p-
387   value<0.01), in 91 cases, *PyLAE* resulted in higher enrichment scores and 41 - in lower scores
388   for African Americans. If the significance cut-off is lowered, *PyLAE* results in a higher number of
389   differentially enriched pathways (Figure 7).
390
391

392   Application of *PyLAE* to African American samples allowed the detection of eleven
393   differentially enriched pathways that were not detected when entire African Americans' genomes
394   were used but appeared when Europeans were compared with Africans from Africa. According to

395 *PyLAE*, the following pathways were enriched in nonsynonymous SNPs: **Africans**: Lipoic acid
396 metabolism, Vitamin B6 metabolism, Fatty acid biosynthesis, Notch signaling pathway, Type I
397 diabetes mellitus, Allograft rejection, Cell adhesion molecules (CAMs), Phagosome, Malaria, Viral
398 myocarditis, HTLV-I infection; **Europeans**: Nitrogen metabolism, Mismatch repair, Cell cycle,
399 Glyoxylate and dicarboxylate metabolism, Porphyrin and chlorophyll metabolism, Insulin
400 resistance, Tight junction, Selenocompound metabolism, Oocyte meiosis, Amyotrophic lateral
401 sclerosis (ALS), Protein digestion and absorption.

402 Dependence on ethnicity efficiency has been reported in processes and conditions related
403 to the above-listed pathways: vitamin B6 metabolism (Gong et al., 2014), fatty acid biosynthesis
404 (Sergeant et al., 2012; Ameur et al., 2012; Kothapalli, Park & Brenna, 2020), resistance to malaria
405 (Singh & Dhar, 2014; Gelabert et al., 2017), the prevalence of viral myocarditis (Shaboodien et
406 al., 2013) and amyotrophic lateral sclerosis (Rechtman et al., 2015; Henning et al., 2021).
407 According to recent studies (Nédélec et al., 2016; Singh et al., 2020), individuals with African
408 ancestry have a stronger inflammatory response and reduced intracellular bacterial growth.
409 Maintaining a strong immune response can have adverse side effects, such as autoimmune
410 disease. Therefore, phagosome efficiency declined after migration out of Africa since Europeans
411 were exposed to fewer pathogens, reducing immune response over generations.
412

413 In summary, *PyLAE* is an easy-to-use, accurate and fast tool for local ancestry analysis
414 that can be used with minimal prior information about the genome or samples.

Availability and requirements

416 Project name: Python Local Admixture Estimation (*PyLAE*)
417 Project home page: https://github.com/smetam/*PyLAE*
418 Operating system(s): Platform independent, Linux is required for pre-processing
419 Programming language: Python, Shell
420 Other requirements: Python 3.5 and higher; bcftools (pre-processing)
421 License: Creative Commons

List of abbreviations

423 AIM - Ancestry Informative Markers
424 GWAS - Genome-Wide Association Study
425 SNP - Single Nucleotide Polymorphism

References

428 Alexander DH, Novembre J, Lange K. 2009. Fast model-based estimation of ancestry in

429 unrelated individuals. *Genome research* 19:1655–1664. DOI: 10.1101/gr.094052.109.

430 Ameur A, Enroth S, Johansson A, Zaboli G, Igl W, Johansson ACV, Rivas MA, Daly MJ,

431 Schmitz G, Hicks AA, Meitinger T, Feuk L, van Duijn C, Oostra B, Pramstaller PP, Rudan I,

432 Wright AF, Wilson JF, Campbell H, Gyllensten U. 2012. Genetic adaptation of fatty-acid

433 metabolism: a human-specific haplotype increasing the biosynthesis of long-chain omega-3

434 and omega-6 fatty acids. *American journal of human genetics* 90:809–820. DOI:

435 10.1016/j.ajhg.2012.03.014.

436 Benítez-Burraco A, Chekalin E, Bruskin S, Tatarinova T, Morozova I. 2021. Recent selection of

437 candidate genes for mammal domestication in Europeans and language change in Europe:

438 a hypothesis. *Annals of human biology* 48:313–320. DOI:

439 10.1080/03014460.2021.1936634.

440 Benjamin DJ, Berger JO, Johannesson M, Nosek BA, Wagenmakers E-J, Berk R, Bollen KA,

441 Brembs B, Brown L, Camerer C, Cesarini D, Chambers CD, Clyde M, Cook TD, De Boeck

442 P, Dienes Z, Dreber A, Easwaran K, Efferson C, Fehr E, Fidler F, Field AP, Forster M,

443 George EI, Gonzalez R, Goodman S, Green E, Green DP, Greenwald AG, Hadfield JD,

444 Hedges LV, Held L, Hua Ho T, Hoijtink H, Hruschka DJ, Imai K, Imbens G, Ioannidis JPA,

445 Jeon M, Jones JH, Kirchler M, Laibson D, List J, Little R, Lupia A, Machery E, Maxwell SE,

446 McCarthy M, Moore DA, Morgan SL, Munafó M, Nakagawa S, Nyhan B, Parker TH,

447 Pericchi L, Perugini M, Rouder J, Rousseau J, Savalei V, Schönbrodt FD, Sellke T, Sinclair

448 B, Tingley D, Van Zandt T, Vazire S, Watts DJ, Winship C, Wolpert RL, Xie Y, Young C,

449 Zinman J, Johnson VE. 2018. Redefine statistical significance. *Nature human behaviour*

450 2:6–10. DOI: 10.1038/s41562-017-0189-z.

451 Browning BL, Zhou Y, Browning SR. 2018. A One-Penny Imputed Genome from Next-

452   Generation Reference Panels. *American journal of human genetics* 103:338–348. DOI:

453   10.1016/j.ajhg.2018.07.015.

454 Chekalin E, Rubanovich A, Tatarinova TV, Kasianov A, Bender N, Chekalina M, Staub K,

455   Koepke N, Rühli F, Bruskin S, Morozova I. 2019. Changes in Biological Pathways During

456   6,000 Years of Civilization in Europe. *Molecular biology and evolution* 36:127–140. DOI:

457   10.1093/molbev/msy201.

458 Cingolani P, Platts A, Wang LL, Coon M, Nguyen T, Wang L, Land SJ, Lu X, Ruden DM. 2012.

459   A program for annotating and predicting the effects of single nucleotide polymorphisms,

460   SnpEff: SNPs in the genome of Drosophila melanogaster strain w1118; iso-2; iso-3. *Fly*

461   6:80–92. DOI: 10.4161/fly.19695.

462 Elhaik E, Tatarinova T, Chebotarev D, Piras IS, Maria Calò C, De Montis A, Atzori M, Marini M,

463   Tofanelli S, Francalacci P, Pagani L, Tyler-Smith C, Xue Y, Cucca F, Schurr TG, Gaieski

464   JB, Melendez C, Vilar MG, Owings AC, Gómez R, Fujita R, Santos FR, Comas D,

465   Balanovsky O, Balanovska E, Zalloua P, Soodyall H, Pitchappan R, Ganeshprasad A,

466   Hammer M, Matisoo-Smith L, Wells RS, Genographic Consortium. 2014. Geographic

467   population structure analysis of worldwide human populations infers their biogeographical

468   origins. *Nature communications* 5:3513. DOI: 10.1038/ncomms4513.

469 Fan S, Kelly DE, Beltrame MH, Hansen MEB, Mallick S, Ranciaro A, Hirbo J, Thompson S,

470   Beggs W, Nyambo T, Omar SA, Meskel DW, Belay G, Froment A, Patterson N, Reich D,

471   Tishkoff SA. 2019. African evolutionary history inferred from whole genome sequence data

472   of 44 indigenous African populations. *Genome Biology* 20. DOI: 10.1186/s13059-019-1679-

473   2.

474 Gelabert P, Olalde I, de-Dios T, Civit S, Lalueza-Fox C. 2017. Malaria was a weak selective

475   force in ancient Europeans. *Scientific Reports* 7. DOI: 10.1038/s41598-017-01534-5.

476 Gong Z, Ambrosone CB, McCann SE, Zirpoli G, Chandran U, Hong C-C, Bovbjerg DH, Jandorf

477   L, Ciupak G, Pawlish K, Lu Q, Hwang H, Khoury T, Wiam B, Bandera EV. 2014.

478   Associations of dietary folate, Vitamins B6 and B12 and methionine intake with risk of

479   breast cancer among African American and European American women. *International*

480   *Journal of Cancer* 134:1422–1435. DOI: 10.1002/ijc.28466.

481 Henning F, Heckmann JM, Naidu K, Vlok L, Cross HM, Marin B. 2021. Incidence of motor

482   neuron disease/amyotrophic lateral sclerosis in South Africa: a 4-year prospective study.

483   *European journal of neurology: the official journal of the European Federation of*

484   *Neurological Societies* 28:81–89. DOI: 10.1111/ene.14499.

485 Hester JM, Wing MR, Li J, Palmer ND, Xu J, Hicks PJ, Roh BH, Norris JM, Wagenknecht LE,

486   Langefeld CD, Freedman BI, Bowden DW, Ng MCY. 2011. Implication of European-derived

487   adiposity loci in African Americans. *International journal of obesity* 36:465–473. DOI:

488   10.1038/ijo.2011.131.

489 Kanehisa M. 2019. Toward understanding the origin and evolution of cellular organisms. *Protein*

490   *Science* 28:1947–1951. DOI: 10.1002/pro.3715.

491 Kanehisa M, Sato Y, Furumichi M, Morishima K, Tanabe M. 2019. New approach for

492   understanding genome variations in KEGG. *Nucleic acids research* 47:D590–D595. DOI:

493   10.1093/nar/gky962.

494 Kantor DB, Palmer CD, Young TR, Meng Y, Gajdos ZK, Lyon H, Price AL, Pollack S, London

495   SJ, Loehr LR, Smith LJ, Kumar R, Jacobs DR Jr, Petrini MF, O'Connor GT, White WB,

496   Papanicolaou G, Burkart KM, Heckbert SR, Barr RG, Hirschhorn JN. 2013. Replication and

497   fine mapping of asthma-associated loci in individuals of African ancestry. *Human genetics*

498   132:1039–1047. DOI: 10.1007/s00439-013-1310-7.

499 Kothapalli KSD, Park HG, Brenna JT. 2020. Polyunsaturated fatty acid biosynthesis pathway

500   and genetics. implications for interindividual variability in prothrombotic, inflammatory

501   conditions such as COVID-19☆,☆☆,★,★★. *Prostaglandins, leukotrienes, and essential*

502   *fatty acids* 162:102183. DOI: 10.1016/j.plefa.2020.102183.

503   Kozlov K, Chebotarev D, Hassan M, Triska M, Triska P, Flegontov P, Tatarinova TV. 2015.

504   Differential Evolution approach to detect recent admixture. *BMC genomics* 16 Suppl 8:S9.

505   DOI: 10.1186/1471-2164-16-S8-S9.

506   Maples BK, Gravel S, Kenny EE, Bustamante CD. 2013. RFMix: a discriminative modeling

507   approach for rapid and robust local-ancestry inference. *American journal of human genetics*

508   93:278–288. DOI: 10.1016/j.ajhg.2013.06.020.

509   Nachman MW, Crowell SL. 2000. Estimate of the mutation rate per nucleotide in humans.

510   *Genetics* 156:297–304. DOI: 10.1093/genetics/156.1.297.

511   N'Diaye A, Chen GK, Palmer CD, Ge B, Tayo B, Mathias RA, Ding J, Nalls MA, Adeyemo A,

512   Adoue V, Ambrosone CB, Atwood L, Bandera EV, Becker LC, Berndt SI, Bernstein L, Blot

513   WJ, Boerwinkle E, Britton A, Casey G, Chanock SJ, Demerath E, Deming SL, Diver WR,

514   Fox C, Harris TB, Hernandez DG, Hu JJ, Ingles SA, John EM, Johnson C, Keating B,

515   Kittles RA, Kolonel LN, Kritchevsky SB, Le Marchand L, Lohman K, Liu J, Millikan RC,

516   Murphy A, Musani S, Neslund-Dudas C, North KE, Nyante S, Ogunniyi A, Ostrander EA,

517   Papanicolaou G, Patel S, Pettaway CA, Press MF, Redline S, Rodriguez-Gil JL, Rotimi C,

518   Rybicki BA, Salako B, Schreiner PJ, Signorello LB, Singleton AB, Stanford JL, Stram AH,

519   Stram DO, Strom SS, Suktitipat B, Thun MJ, Witte JS, Yanek LR, Ziegler RG, Zheng W,

520   Zhu X, Zmuda JM, Zonderman AB, Evans MK, Liu Y, Becker DM, Cooper RS, Pastinen T,

521   Henderson BE, Hirschhorn JN, Lettre G, Haiman CA. 2011. Identification, replication, and

522   fine-mapping of Loci associated with adult height in individuals of african ancestry. *PLoS*

523   *genetics* 7:e1002298. DOI: 10.1371/journal.pgen.1002298.

524   Nédélec Y, Sanz J, Baharian G, Szpiech ZA, Pacis A, Dumaine A, Grenier J-C, Freiman A,

525   Sams AJ, Hebert S, Pagé Sabourin A, Luca F, Blekhman R, Hernandez RD, Pique-Regi R,

526   Tung J, Yotova V, Barreiro LB. 2016. Genetic Ancestry and Natural Selection Drive

527   Population Differences in Immune Responses to Pathogens. *Cell* 167:657–669.e21. DOI:

528   10.1016/j.cell.2016.09.025.

529   Ogata H, Goto S, Sato K, Fujibuchi W, Bono H, Kanehisa M. 1999. KEGG: Kyoto Encyclopedia

530   of Genes and Genomes. *Nucleic acids research* 27:29–34. DOI: 10.1093/nar/27.1.29.

531   Pasaniuc B, Sankararaman S, Kimmel G, Halperin E. 2009. Inference of locus-specific ancestry

532   in closely related populations. *Bioinformatics* 25:i213–21. DOI:

533   10.1093/bioinformatics/btp197.

534   Rechtman L, Jordan H, Wagner L, Horton DK, Kaye W. 2015. Racial and ethnic differences

535   among amyotrophic lateral sclerosis cases in the United States. *Amyotrophic lateral*

536   *sclerosis & frontotemporal degeneration* 16:65–71. DOI: 10.3109/21678421.2014.971813.

537   Sankararaman S, Sridhar S, Kimmel G, Halperin E. 2008. Estimating local ancestry in admixed

538   populations. *American journal of human genetics* 82:290–303. DOI:

539   10.1016/j.ajhg.2007.09.022.

540   Sergeant S, Hugenschmidt CE, Rudock ME, Ziegler JT, Ivester P, Ainsworth HC, Vaidya D,

541   Case LD, Langefeld CD, Freedman BI, Bowden DW, Mathias RA, Chilton FH. 2012.

542   Differences in arachidonic acid levels and fatty acid desaturase (FADS) gene variants in

543   African Americans and European Americans with diabetes or the metabolic syndrome. *The*

544   *British journal of nutrition* 107:547–555. DOI: 10.1017/S0007114511003230.

545   Shaboodien G, Maske C, Wainwright H, Smuts H, Ntsekhe M, Commerford PJ, Badri M, Mayosi

546   BM. 2013. Prevalence of myocarditis and cardiotropic virus infection in Africans with HIV-

547   associated cardiomyopathy, idiopathic dilated cardiomyopathy and heart transplant

548   recipients: a pilot study: cardiovascular topic. *Cardiovascular journal of Africa* 24:218–223.

549   DOI: 10.5830/CVJA-2013-039.

550   Singh V, Dhar PK. 2014. *Systems and Synthetic Biology*. Springer.

551   Singh KS, Leu JI-J, Barnoud T, Vonteddu P, Gnanapradeepan K, Lin C, Liu Q, Barton JC,

552   Kossenkov AV, George DL, Murphy ME, Dotiwala F. 2020. African-centric TP53 variant

553   increases iron accumulation and bacterial pathogenesis but improves response to malaria

554   toxin. *Nature Communications* 11. DOI: 10.1038/s41467-019-14151-9.

555   Skoglund P, Thompson JC, Prendergast ME, Mittnik A, Sirak K, Hajdinjak M, Salie T, Rohland

556   N, Mallick S, Peltzer A, Heinze A, Olalde I, Ferry M, Harney E, Michel M, Stewardson K,

557   Cerezo-Román JI, Chiumia C, Crowther A, Gomani-Chindebvu E, Gidna AO, Grillo KM,

558   Taneli Helenius I, Hellenthal G, Helm R, Horton M, López S, Mabulla AZP, Parkington J,

559   Shipton C, Thomas MG, Tibesasa R, Welling M, Hayes VM, Kennett DJ, Ramesar R,

560   Meyer M, Pääbo S, Patterson N, Morris AG, Boivin N, Pinhasi R, Krause J, Reich D. 2017.

561   Reconstructing Prehistoric African Population Structure. *Cell* 171:59–71.e21. DOI:

562   10.1016/j.cell.2017.08.049.

563   Sudmant PH, Rausch T, Gardner EJ, Handsaker RE, Abyzov A, Huddleston J, Zhang Y, Ye K,

564   Jun G, Fritz MH-Y, Konkel MK, Malhotra A, Stütz AM, Shi X, Casale FP, Chen J,

565   Hormozdiari F, Dayama G, Chen K, Malig M, Chaisson MJP, Walter K, Meiers S, Kashin S,

566   Garrison E, Auton A, Lam HYK, Mu XJ, Alkan C, Antaki D, Bae T, Cerveira E, Chines P,

567   Chong Z, Clarke L, Dal E, Ding L, Emery S, Fan X, Gujral M, Kahveci F, Kidd JM, Kong Y,

568   Lameijer E-W, McCarthy S, Flicek P, Gibbs RA, Marth G, Mason CE, Menelaou A, Muzny

569   DM, Nelson BJ, Noor A, Parrish NF, Pendleton M, Quitadamo A, Raeder B, Schadt EE,

570   Romanovitch M, Schlattl A, Sebra R, Shabalin AA, Untergasser A, Walker JA, Wang M, Yu

571   F, Zhang C, Zhang J, Zheng-Bradley X, Zhou W, Zichner T, Sebat J, Batzer MA, McCarroll

572   SA, 1000 Genomes Project Consortium, Mills RE, Gerstein MB, Bashir A, Stegle O, Devine

573   SE, Lee C, Eichler EE, Korbel JO. 2015. An integrated map of structural variation in 2,504

574   human genomes. *Nature* 526:75–81. DOI: 10.1038/nature15394.

575   Tatarinova T, Bouck J, Schumitzky A. 2008. Kullback-Leibler Markov chain Monte Carlo--a new

576   algorithm for finite mixture analysis and its application to gene expression data. *Journal of*

577   *bioinformatics and computational biology* 6:727–746. DOI: 10.1142/s0219720008003710.

578   Tatarinova TV, Schumitzky A. 2014. *Nonlinear Mixture Models: A Bayesian Approach*. World

579   Scientific.

580   Uren C, Hoal EG, Möller M. 2020. Putting RFMix and ADMIXTURE to the test in a complex

581   admixed population. *BMC genetics* 21:40. DOI: 10.1186/s12863-020-00845-3.

582   Viterbi A. 1967. Error bounds for convolutional codes and an asymptotically optimum decoding

583   algorithm. *IEEE Transactions on Information Theory* 13:260–269. DOI:

584   10.1109/tit.1967.1054010.

585   Wang K, Li M, Hakonarson H. 2010. ANNOVAR: functional annotation of genetic variants from

586   high-throughput sequencing data. *Nucleic acids research* 38:e164. DOI:

587   10.1093/nar/gkq603.

588   Yang H, Wang K. 2015. Genomic variant annotation and prioritization with ANNOVAR and

589   wANNOVAR. *Nature protocols* 10:1556–1566. DOI: 10.1038/nprot.2015.105.

590

Figure 1

Admixture plots for worldwide individuals from 1000 Genomes project.

Top: diploid mode. Bottom: haploid mode. Colors: Red - North-East Asian, Orange - Mediterranean, Light green - South African, Dark green - South-West Asian, Light blue - Native American, Blue - Oceanian, Dark blue - Southeast Asian, Purple - Northern European, Magenta - Sub-Saharan African.
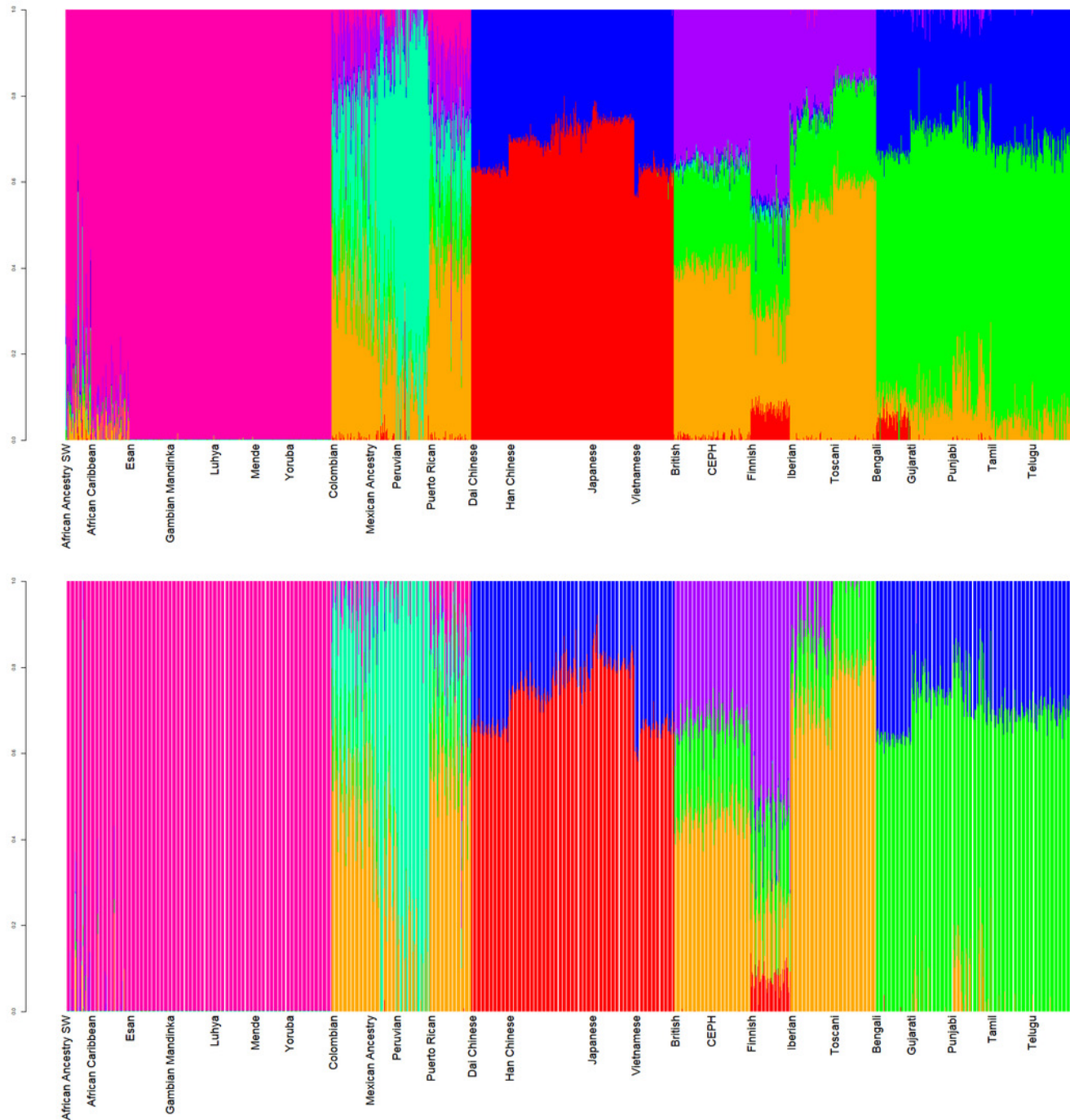
Figure 2

Clustered Admixture plot for worldwide individuals from 1000 Genomes project.

Clustered Admixture for 10000 Genomes individuals. Top: diploid mode. Bottom: haploid mode. Colors: Red - North-East Asian, Orange - Mediterranean, Light green - South African, Dark green - South-West Asian, Light blue - Native American, Blue - Oceanian, Dark blue - Southeast Asian, Purple - Northern European, Magenta - Sub-Saharan African.
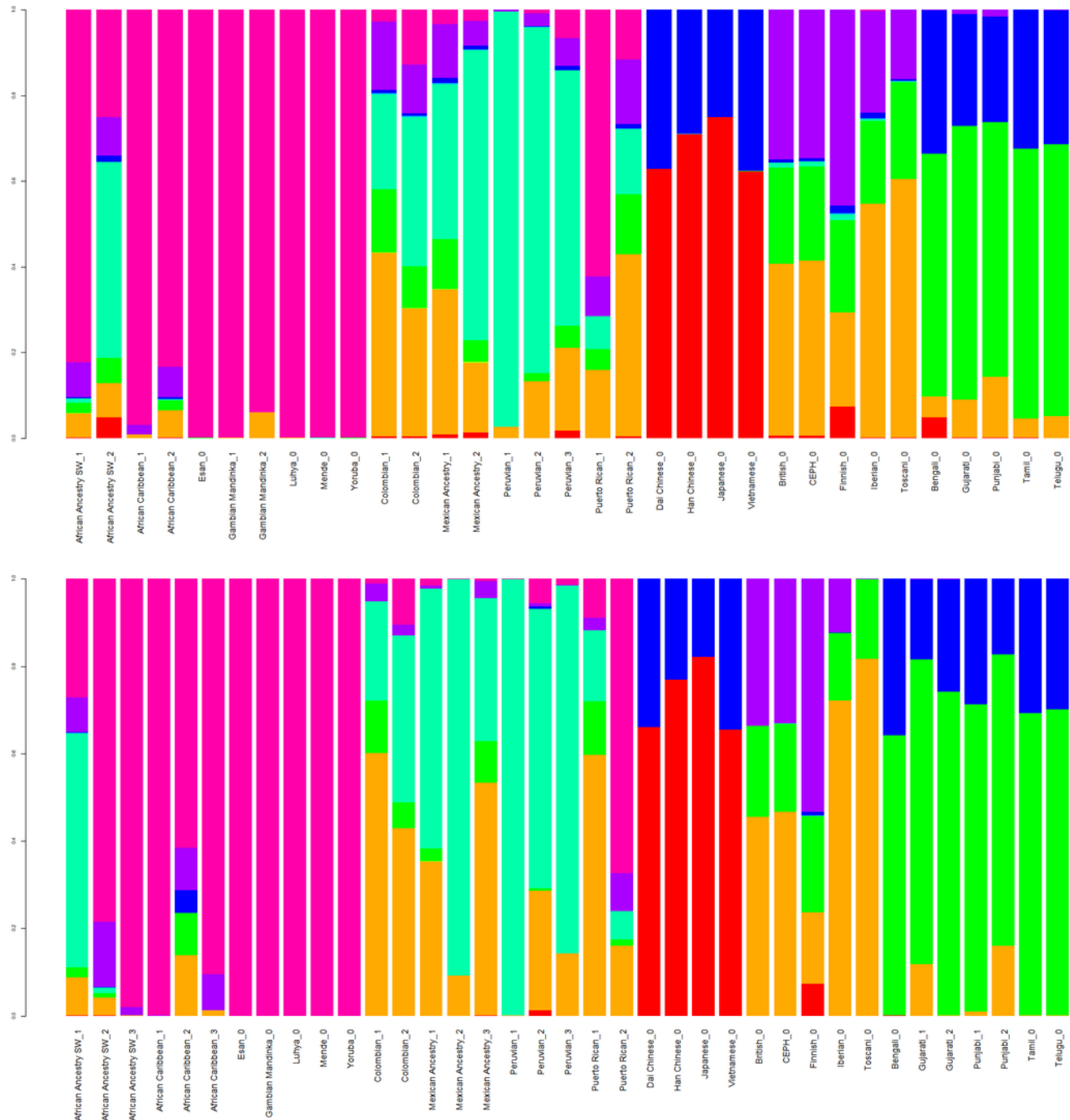
Figure 3

Difference between the largest admixture component in the aggregated haploid and diploid cases.

We have identified the largest admixture component for every sample and calculated the difference between the average parental value of this component and its diploid value. The mean difference was 0.0684, indicating that haploid admixture tends to slightly increase the value of the largest component determined by the diploid mode.
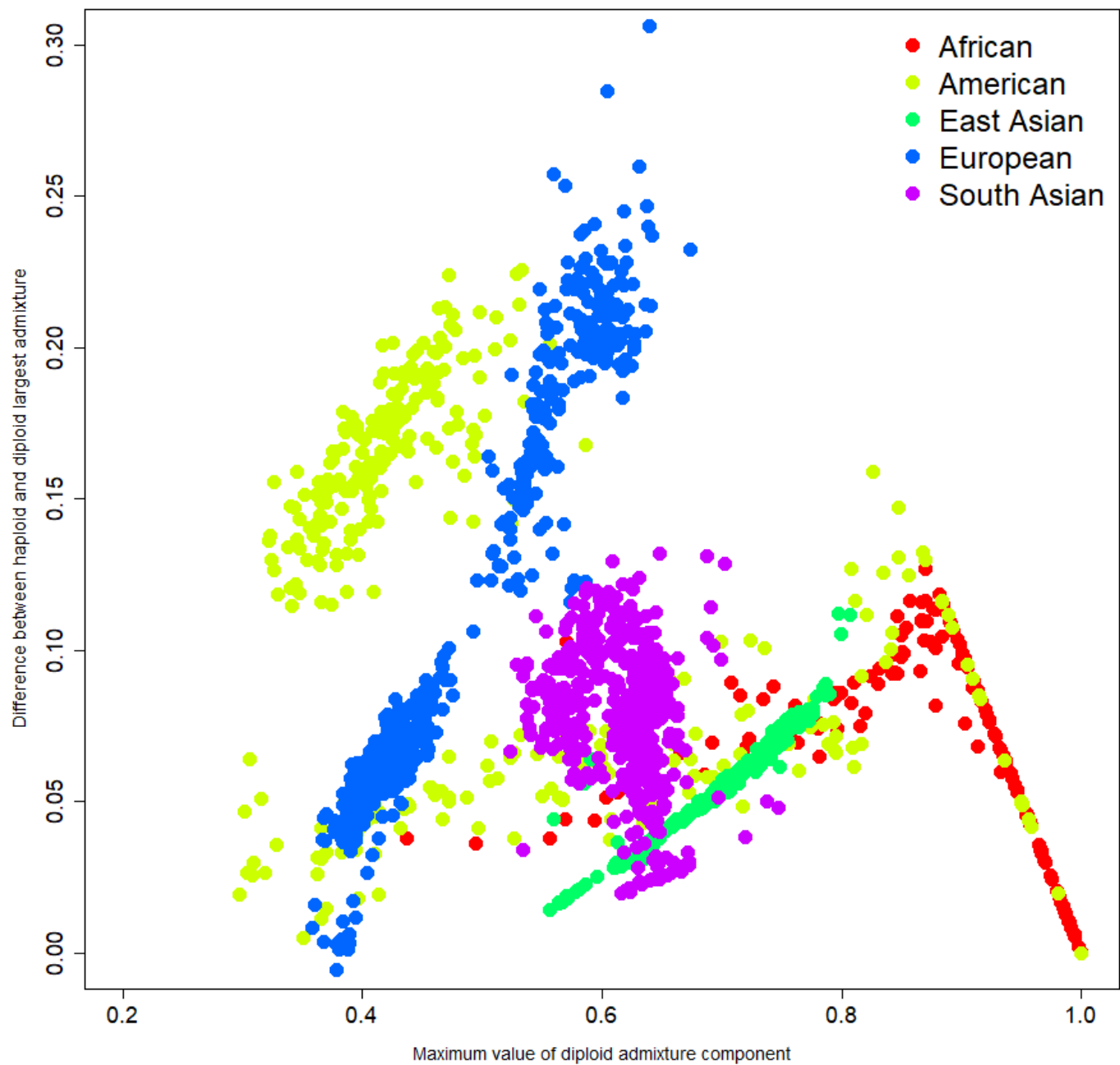
Figure 4

ReAdmix assignment matrix heatmap

reAdmix analysis shows that population labels may not be 100% accurate, however, they are correct at the superpopulation level. This may be explained by the presence of admixed individuals in the dataset, and by shared histories by various groups. The assignment matrix indicates the percentage assignment. The color intensity of the heatmap shows the probability of an individual from a reference population (columns) being assigned to a given population (rows). The darkest shade indicates the highest probability and the lightest shade indicates the lowest.
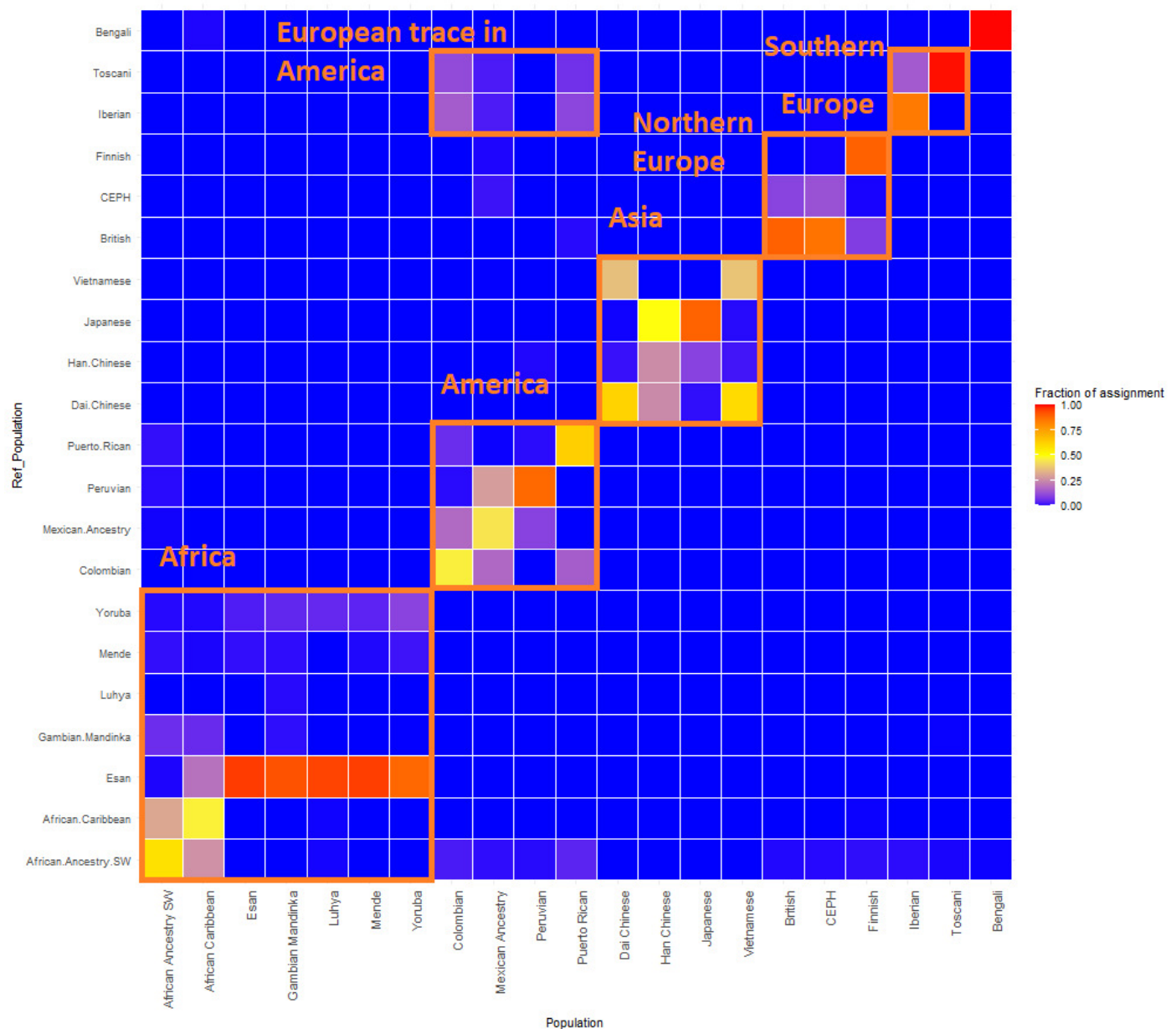
Figure 5

Histograms of euclidean distances of aggregated PyLAE results vs. admixture vectors.

Euclidean distances of aggregated PyLAE results vs. admixture vectors for 2,504 from 1000 Genomes. A. 'Haploid' mode, no admixture prior B. 'Haploid' mode, with admixture prior C. "Diploid" mode, no admixture prior D. "Diploid" mode, with admixture prior.
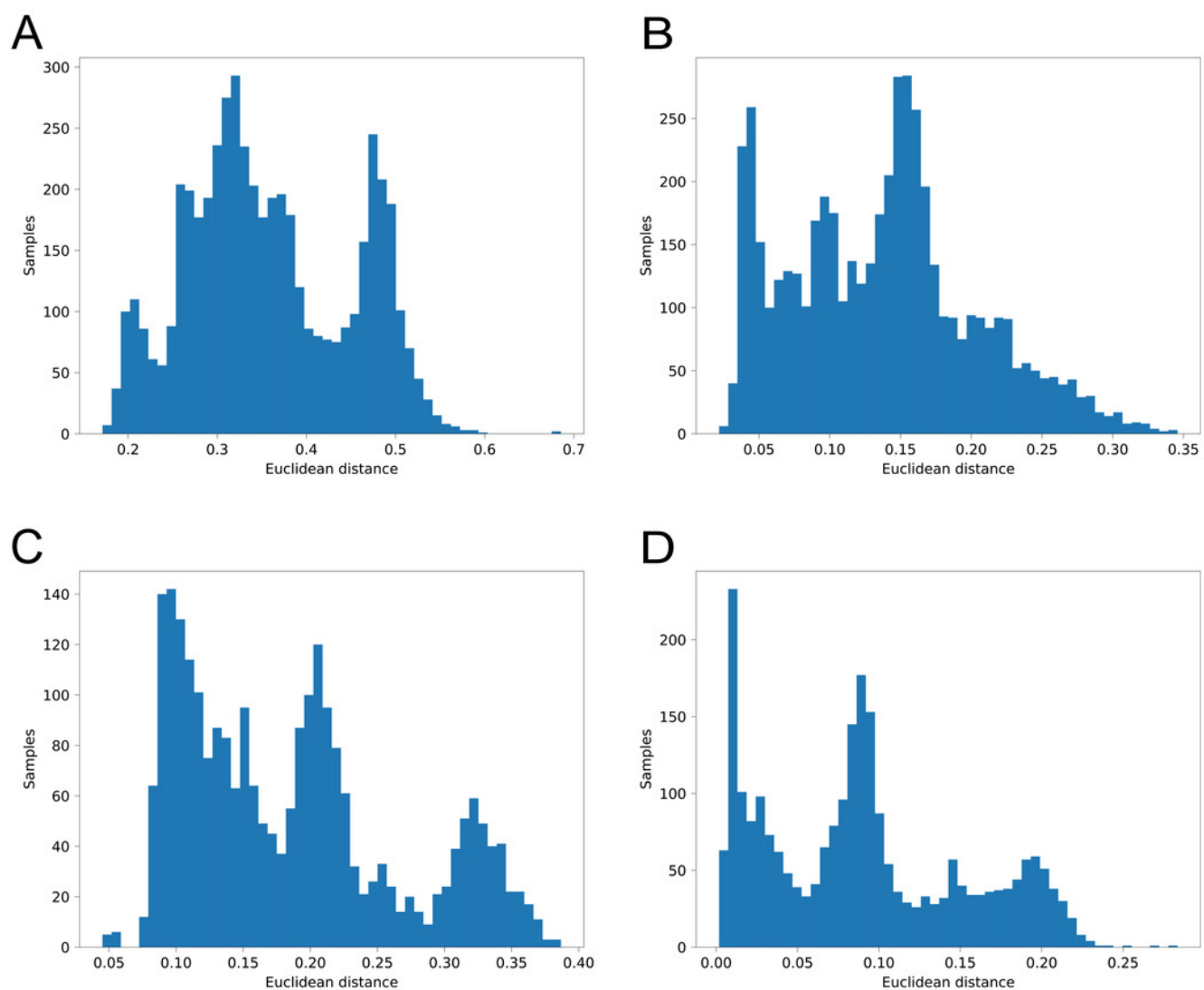
Figure 6

Comparison of performance of PyLAE and RFMix using 1000 Genomes database.

Four PyLAE runs were performed: 15, 30, 50, and 100 SNP windows. RFMix program was used with default parameters. Euclidean distance was computed between the Admixture profiles and predicted aggregated ancestry for TSI (A) and CLM (B) samples.
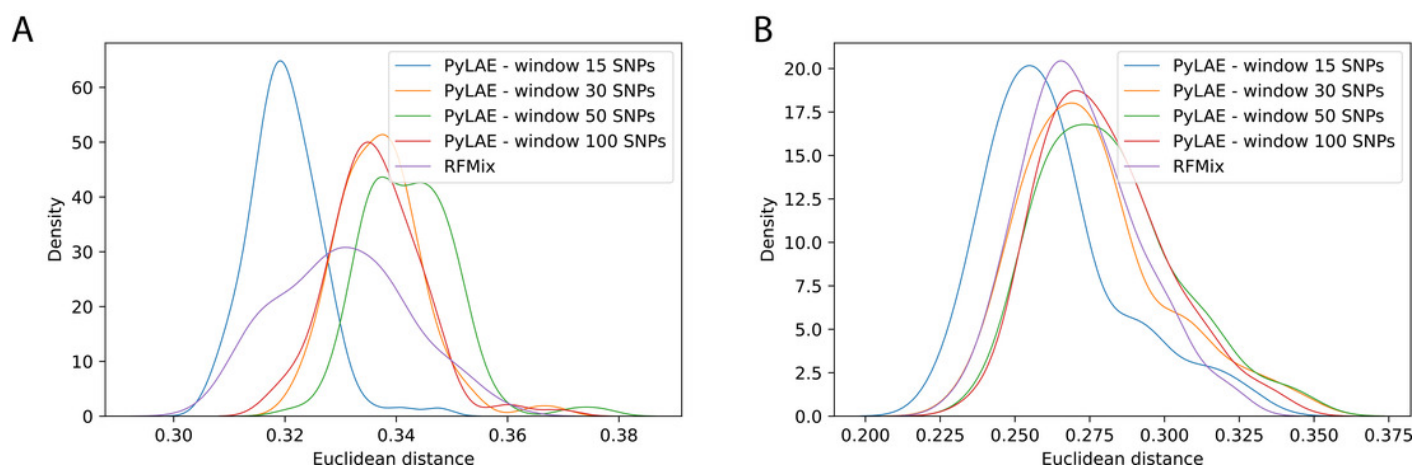
Figure 7

Fraction of significantly enriched pathways as a function of a significance cut-off.

PyLAE has higher enrichment scores compared to the whole-genome approach. Comparing the enrichment scores between differentially enriched pathways (p-value<0.01), in 91 cases, PyLAE resulted in higher enrichment scores and 41 - in lower sc.ores for African Americans. If the significance cut-off is lowered, PyLAE results in a higher number of differentially enriched pathways
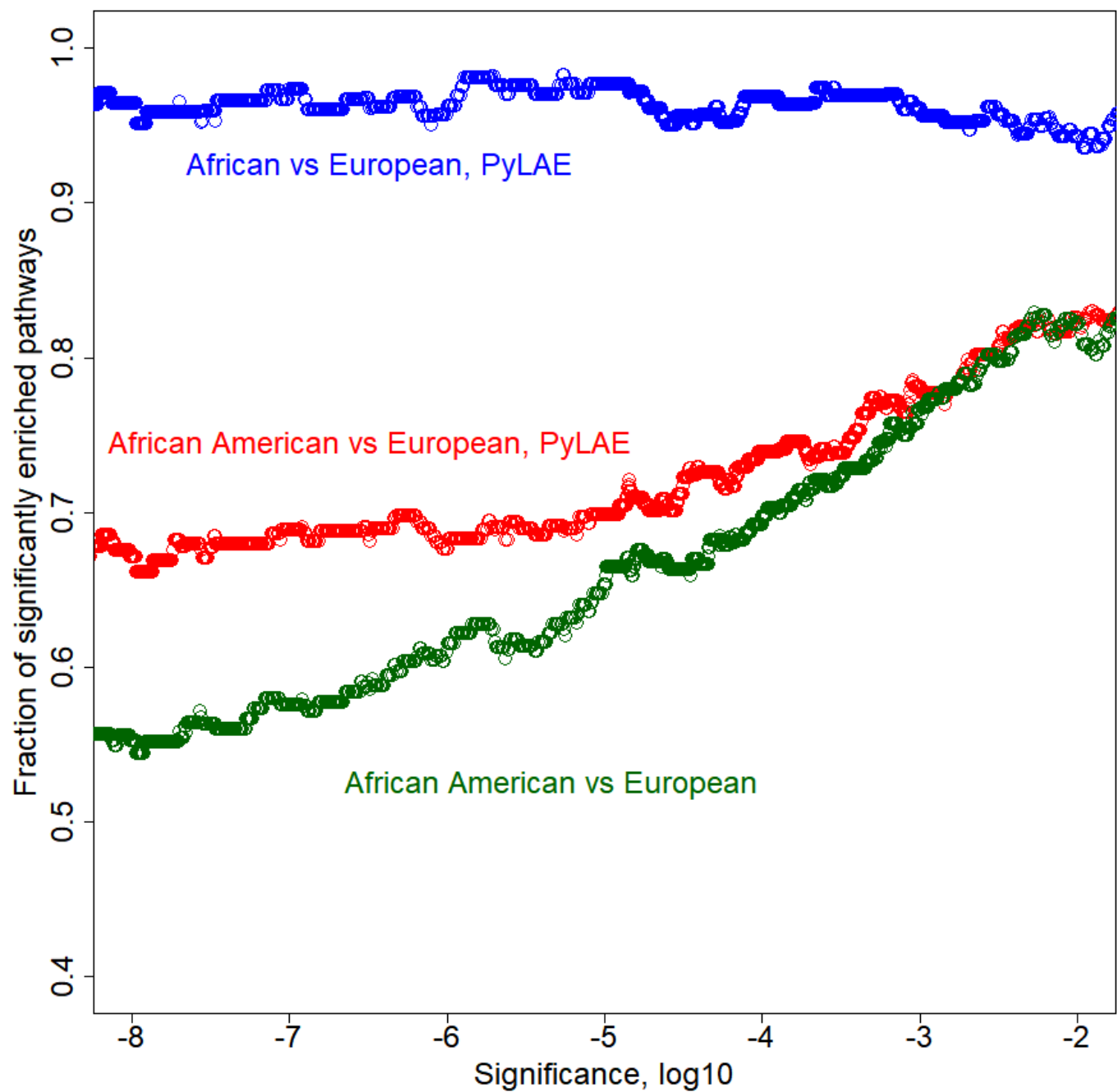
Clusters of admixture vector clusters for 1000 Genomes individuals.

Admixture vectors were obtained using Admixture in supervised mode.

Superpopulation name	Cluster	NorthEastAsian	Mediterranean	SouthAfrican	SouthWestAsian	NativeAmerican	Oceanian	SouthEastAsian	NorthernEuropean	SubsaharanAfrican	#ind
African	African Ancestry SW_1	5%	8%	0%	6%	46%	0%	1%	9%	25%	3
	African Ancestry SW_2	0%	6%	0%	2%	1%	0%	0%	8%	82%	58
	African Caribbean_1	0%	6%	0%	2%	0%	0%	1%	7%	83%	35
	African Caribbean_2	0%	1%	0%	0%	0%	0%	0%	2%	97%	61
	Esan_0	0%	0%	0%	0%	0%	0%	0%	0%	100%	99
	Gambian Mandinka_1	0%	0%	0%	0%	0%	0%	0%	0%	100%	112
	Gambian Mandinka_2	0%	6%	0%	0%	0%	0%	0%	0%	94%	1
	Luhya_0	0%	0%	0%	0%	0%	0%	0%	0%	100%	99
	Mende_0	0%	0%	0%	0%	0%	0%	0%	0%	100%	85
	Yoruba_0	0%	0%	0%	0%	0%	0%	0%	0%	100%	108
American Ancestry	Colombian_1	0%	43%	0%	15%	22%	0%	1%	16%	3%	50
	Colombian_2	0%	30%	0%	10%	35%	0%	1%	11%	13%	40
	Mexican Ancestry_1	1%	16%	0%	5%	68%	0%	1%	6%	3%	27
	Mexican Ancestry_2	1%	34%	0%	12%	36%	0%	1%	13%	3%	37
	Peruvian_1	0%	3%	0%	0%	97%	0%	0%	0%	0%	25
	Peruvian_2	2%	19%	0%	5%	60%	0%	1%	7%	7%	27
	Peruvian_3	0%	13%	0%	2%	81%	0%	0%	3%	1%	33
	Puerto Rican_1	0%	42%	0%	14%	15%	0%	1%	15%	12%	90
	Puerto Rican_2	0%	16%	0%	5%	8%	0%	0%	9%	62%	3
East Asian	Dai Chinese_0	63%	0%	0%	0%	0%	0%	37%	0%	0%	92
	Han Chinese_0	71%	0%	0%	0%	0%	0%	29%	0%	0%	197
	Japanese_0	75%	0%	0%	0%	0%	0%	25%	0%	0%	104
	Vietnamese_0	62%	0%	0%	0%	0%	0%	38%	0%	0%	99
European	British_0	1%	40%	0%	22%	1%	0%	1%	35%	0%	91
	CEPH_0	1%	41%	0%	22%	1%	0%	1%	35%	0%	99
	Finnish_0	7%	22%	0%	22%	1%	0%	2%	46%	0%	93

	Iberian_0	0%	55%	0%	19%	0%	0%	1%	24%	0%	107
	Toscani_0	0%	60%	0%	23%	0%	0%	0%	16%	0%	107
South Asian	Bengali_0	5%	5%	0%	57%	0%	0%	33%	0%	0%	86
	Gujarati_0	0%	9%	0%	64%	0%	0%	26%	1%	0%	103
	Punjabi_0	0%	14%	0%	60%	0%	0%	25%	2%	0%	96
	Tamil_0	0%	4%	0%	63%	0%	0%	32%	0%	0%	102
	Telugu_0	0%	5%	0%	64%	0%	0%	31%	0%	0%	102

Haploid admixture vector clusters for 1000 Genomes individuals

Supervised admixture using phased haploid data

Superpopulation name	Cluster	NorthEastAsian	Mediterranean	SouthAfrican	SouthWestAsian	NativeAmerican	Oceanian	SouthEastAsian	Northern European	SubsaharanAfrican	#parents
African	African Ancestry SW_1	0%	0%	0%	0%	0%	0%	0%	2%	98%	71
	African Ancestry SW_2	0%	4%	0%	1%	1%	0%	0%	15%	78%	45
	African Ancestry SW_3	0%	9%	0%	2%	54%	0%	0%	8%	27%	6
	African Caribbean_1	0%	14%	0%	10%	0%	0%	5%	10%	62%	6
	African Caribbean_2	0%	1%	0%	0%	0%	0%	0%	8%	90%	26
	African Caribbean_3	0%	0%	0%	0%	0%	0%	0%	0%	100%	160
	Esan_0	0%	0%	0%	0%	0%	0%	0%	0%	100%	198
	Gambian Mandinka_0	0%	0%	0%	0%	0%	0%	0%	0%	100%	226
	Luhya_0	0%	0%	0%	0%	0%	0%	0%	0%	100%	198
	Mende_0	0%	0%	0%	0%	0%	0%	0%	0%	100%	170
	Yoruba_0	0%	0%	0%	0%	0%	0%	0%	0%	100%	216
American	Colombian_1	0%	43%	0%	6%	38%	0%	0%	2%	11%	86
	Colombian_2	0%	60%	0%	12%	22%	0%	0%	4%	1%	94
	Mexican Ancestry_1	0%	35%	0%	3%	59%	0%	0%	1%	2%	60
	Mexican Ancestry_2	0%	53%	0%	10%	33%	0%	0%	4%	1%	46
	Mexican Ancestry_3	0%	9%	0%	0%	91%	0%	0%	0%	0%	22
	Peruvian_1	1%	27%	0%	1%	64%	0%	1%	1%	6%	48
	Peruvian_2	0%	14%	0%	0%	84%	0%	0%	0%	1%	50
	Peruvian_3	0%	0%	0%	0%	100%	0%	0%	0%	0%	72
	Puerto Rican_1	0%	59%	0%	12%	16%	0%	0%	3%	10%	180
	Puerto Rican_2	0%	16%	0%	1%	6%	0%	0%	9%	67%	6
East Asian	Dai Chinese_0	66%	0%	0%	0%	0%	0%	34%	0%	0%	184
	Han Chinese_0	77%	0%	0%	0%	0%	0%	23%	0%	0%	394
	Japanese_0	82%	0%	0%	0%	0%	0%	18%	0%	0%	208
	Vietnamese_0	65%	0%	0%	0%	0%	0%	35%	0%	0%	198

European	British_0	0%	46%	0%	21%	0%	0%	0%	34%	0%	182
	CEPH_0	0%	47%	0%	20%	0%	0%	0%	33%	0%	198
	Finnish_0	7%	17%	0%	22%	0%	0%	1%	53%	0%	186
	Iberian_0	0%	72%	0%	16%	0%	0%	0%	12%	0%	214
	Toscani_0	0%	82%	0%	18%	0%	0%	0%	0%	0%	214
South Asian	Bengali_0	0%	0%	0%	64%	0%	0%	36%	0%	0%	172
	Gujarati_1	0%	0%	0%	74%	0%	0%	26%	0%	0%	180
	Gujarati_2	0%	12%	0%	70%	0%	0%	18%	0%	0%	26
	Punjabi_1	0%	16%	0%	67%	0%	0%	17%	0%	0%	89
	Punjabi_2	0%	1%	0%	70%	0%	0%	29%	0%	0%	103
	Tamil_0	0%	0%	0%	69%	0%	0%	31%	0%	0%	204
	Telugu_0	0%	0%	0%	70%	0%	0%	30%	0%	0%	204

GPS and reAdmix

Results of GPS and reAdmix analyses. For each population, we report factions of self-hits (when the tool correctly identifies the population label) and superpopulation hits (when a superpopulation is correctlyidentified).

Super-Population	Population	Number of individuals	GPS, Fraction of populations self-hits	GPS, Fraction of super-population hits	reAdmix, Fraction of populations self-hits	reAdmix, Fraction of super-population hits
African	African Ancestry SW	61	0.34	0.85	0.58	0.98
	African Caribbean	96	0.56	0.97	0.47	0.99
	Esan	99	0.07	1.00	0.96	1.00
	Gambian Mandinka	113	0.01	1.00	0.01	1.00
	Luhya	99	0.07	1.00	0.00	1.00
	Mende	85	0.92	1.00	0.01	1.00
	Yoruba	108	0.19	1.00	0.10	1.00
American	Colombian	94	0.65	0.96	0.46	0.70
	Mexican Ancestry	64	0.5	0.97	0.17	0.89
	Peruvian	85	0.8	0.98	0.86	0.96
	Puerto Rican	104	0.85	0.93	0.63	0.78
East Asian	Dai Chinese	93	0.62	1.00	0.62	1.00
	Han Chinese	208	0.71	1.00	0.25	1.00
	Japanese	104	0.96	1.00	0.89	1.00
	Vietnamese	99	0.41	1.00	0.37	1.00
European	British	91	0.58	1.00	0.89	0.99

	CEPH	99	0.57	1.00	0.13	0.99
	Finnish	99	0.97	1.00	0.90	0.99
	Iberian	107	0.94	1.00	0.84	0.98
	Toscani	107	1	1.00	0.99	0.99
Southeast Asian	Bengali	86	0.9	1.00	0.72	1.00
	Gujarati	103	0.69	1.00	0.52	0.99
	Punjabi	96	0.59	1.00	0.46	0.98
	Tamil	102	0.59	1.00	0.73	1.00
	Telugu	102	0.34	1.00	0.34	1.00

Average Euclidean distance between global admixture vectors and aggregated PyLAE results in diploid mode.

Accuracy of PyLAE is assessed using the difference between aggregated results predicted by PyLAE and independently calculated admixture vector.

	Average Euclidean distance between the global admixture vector and aggregated PyLAE results in diploid mode	
Population	Informative prior	Uniform prior
Yoruba	0.000747008	0.013042043
Esan	0.000770357	0.013533177
Mende	0.000856896	0.018231929
Iberian	0.001331954	0.012167398
Gambian Mandinka	0.001365033	0.021373737
Toscani	0.001539027	0.019696897
Luhya	0.001826951	0.027512649
African Caribbean	0.004803319	0.0301569
Puerto Rican	0.005675916	0.017629195
CEPH	0.006072862	0.011648137
Japanese	0.006491083	0.046715682
British	0.006925157	0.012265145
Han Chinese	0.007304674	0.045295263
Kinh	0.007519174	0.04711133
Southern Han Chinese	0.0075584	0.044229833
Dai Chinese	0.008293571	0.051361167
Kinh Vietnamese	0.008600211	0.05305063
African Ancestry SW	0.010087603	0.03448744
Colombian	0.01190426	0.030931471
Peruvian	0.016376169	0.069468746
Mexican Ancestry	0.018915794	0.049218005
Finnish	0.02410449	0.038832151
Punjabi	0.026287313	0.08384595
Gujarati	0.028881709	0.093738688
Telugu	0.033376937	0.115691247
Tamil	0.036767906	0.120281378
Bengali	0.04353631	0.110281922

Pearson correlation coefficients between aggregated local ancestry predictions by PyLAE and RFMix and global ancestry, represented by Admixture vectors.

For individuals with East Asian and European ancestry, PyLAE has a higher correlation with corresponding global ancestral composition compared to RFMix, while for African, American, and South Asian individuals, RFMix had a higher correlation. It is important to notice that global and aggregated local ancestries were in agreement for both programs; the lowest correlation coefficient was 0.8676.

1   *Table 5. Pearson correlation coefficients between aggregated local ancestry predictions by PyLAE and RFMix and*
2   *global ancestry, represented by Admixture vectors.*

Superpopulation	PyLAE	RFMix
AFR	0.9893	0.9996
AMR	0.9675	0.9851
EAS	0.9783	0.9684
EUR	0.9744	0.9699
SAS	0.9185	0.9595